Chapter 4

Polyurethane-chitosan based brush copolymer as injectable hydrogel for controlled drug delivery

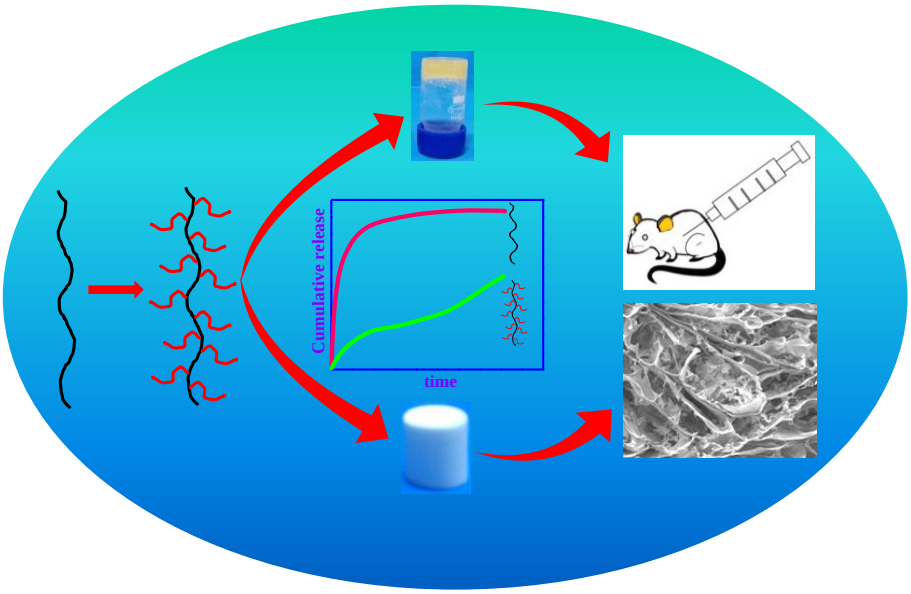

Mahanta et al., ***Polym. Chem.*, 2017, 8, 6233-6249**

4.1 Introduction

A large number of therapeutics has been discovered but very few of them have shown clinical success. The low performance of most drug delivery vehicles depends on the several factors such as low bioavailability, the extent and the rate at which a drug reaches and affects the target tissue [Kidane et al. 2005].These factors are related to the route of administration, organ physiology and metaboloism [Wang et al. 2005]. After administration of drug regularly, bioavailability of drug is very low and drug concentration in blood plasma can drop very quickly below therapeutic window requiring an overdose which decreases patient's compliance [Bhattarai et al. 2010]. To cope with this situation controlled drug delivery system is an alternating approach to regulate the bioavailability of drugs. Controlled drug delivery system release the drug in predefined manner within therapeutic window [Wise et al. 2000; Jogani et al., 2008]. Several drug delivery systems have been developed based on synthetic and natural polymers by incorporating drug into the polymer network structure. Polymeric drug delivery matrices have great advantages because of their wide-range hydrophobic and/orhydrophilic components and their polymer-polymer, polymer-drug, polymer-solvent, or polymer-physiological medium interactions. Although several combination of materials have been designed but their engineering is restricted by materials biocompatibility, toxic byproducts, surgical removal of drug delivery system and manufacturing cost [Hoffman et al., 2002].

Researchers have found that hydrogels have the ability to serve as versatile and viable platforms for drug delivery systems [Hoffman et al., 2002; Peppas et al., 2006]. Hydrogels are three dimensional polymeric networks having the capability to absorb large amount of water maintaining their structural integrity [Wei et al., 2016]. Hydrogels have been widely used in tissue engineering and drug delivery as they can

mimic as extracellular matrix because of their high water content [Wu et al., 2015; Liu et al., 2015]. Porous scaffold are also used for the similar purpose as they can serve as a template for host infiltration and physical support to guide the growth and proliferation of cells into the targeted functional tissue or organ [Gao et al., 2003; Peter et al., 2010].

There are several literature reports on hydrogel drug delivery system using synthetic hydrophilic polymers, but major drawbacks are many of them are not biodegradable (poly(N-isopropyl acrylamide), poly(2-hydroxyethyl methacrylate), poly(vinyl alcohol)) or suffer from other issues, such as local inflammation etc [Hoffman et al., 2002; Ganta et al., 2008, Hamidi et al., 2008; Wichterle et al., 1960; Qiu et al., 2001]. Biocompatible and biodegradable hydrogels have been developed using synthetic polymers containing hydrolyzable moieties or using natural polymers that are susceptible towards enzymatic degradation. Now a days, a great attention have been paid to the hydrogel designed from natural polymer Chitosan because of their well documented biocompatibility, low toxicity and degradability by human enzymes [Knapczyk et al., 1989; Hirano et al., 1990; Muzzarelli et al., 1997; Zhao et al., 2015; Zhao et al., 2017]. Chitosan a naturally occurring biopolymers obtained from the deacetylation of chitin that finds wide applications in biomedical fields [Jiang et al., 2014; Chen et al., 2014; Qi et al., 2015; Mahanta et al., 2016; Rinaudo et al., 2006;]. It is a cationic polysaccharide and a copolymer of β-(1,4) linked 2-acetamido-2-deoxy-D-glucopyranose and 2-amino-2-deoxy-D-glucopyronose. Polyurethanes (PUs) are also drawing great attention as synthetic polymers have been extensively used in biomedical applications and various industries especially motor vehicles [Zia et al., 2014; Wu et al., 2016; Chen et al., 2015]. Now a days, PUs are heavily used in biomedical fields instead ofother synthetic and natural polymers such as natural rubber, poly (vinyl chloride), fluoropolymers, polyethylene and silicones because of their interesting mechanical properties and

relatively better biocompatibility [Brook et al., 2006; Greene et al., 2005; Zia et al., 2009]. PUs behaves as part of human body as urethane linkage presents in PUs is analogous to the peptide linkage that presents in protein. PUs are used in making absorbable and non-absorbable sutures, heart valves, aortic grafts, dialysis membranes, insulation pacemaker electrodes, catheters, intra-aortic balloons and breast implants because of these unique properties [Lelah et al., 1986]. Biocompatible nature of PUs can be enhanced by introducing polysaccharides, such as chitosan, chitin and starch moieties as a chain extender. Chitosan contain active two –OH groups located at C_3 and C_6 position and one $–NH_2$ group at C_2 position in its backbone which are very susceptible to chemically react with PU prepolymer to produce chitosan based polyurethane. To best of our knowledge there is not enough comprehensive reports on the molecular engineering of chitosan based polyurethane hydrogel for controlled drug delivery and tissue engineering purpose.

In this chapter, we have focused in the development of chitosan based polyurethane brush hydrogel for controlling drug delivery in a sustained manner and tissue engineering purpose. Hydrophilic nature of the chitosan is controlled through grafting of polyurethane prepolymer on chitosan backbone. Grafting is confirmed through different spectroscopic technique including ^{13}C solid state NMR, FTIR and UV-visible. Hydrophobic modification of Chitosan is observed through swelling study and contact angle measurement. Hydrogels are developed with the pure chitosan and its graft copolymer in diluted acetic acid medium. Scaffolds are also designed from the hydrogel through lyophilization technique. Structure and Structure and morphology of the hydrogels are illustrated in this context. Sustainable drug release kinetics behavior is achieved using both hydrogel and scaffolds. Drug release behavior can also be tuned by controlling the degree of substitution. Cytotoxicity of the hydrogel and scaffold is

checked using NIH 3T3 mouse embryonic fibroblast cells. In vivo gelation study is performed using brush like copolymer to demonstrate its use as injectable hydrogel. Henceforth, hydrogel and scaffold of the brush like copolymer has the tremendous potential for biomedical application.

4.2 Results and discussion

4.2.1 Formation of brush copolymer and interactions

Polyurethane chains are grafted onto Chitosan back bone with different degree of substitution (DS).^{13}C solid state NMR spectroscopic technique confirms the grafting phenomena. **Figure 4.2a** represents the NMR spectra of pure CHT and its graft copolymers. Peaks are assigned from the literature reports [Shao et al., 2016; Khan et al., 2011; Oliveria et al., 2012]. Chitosan contains reactive functional $–NH_2$ and –OH groups located at C_2 and C_6 position which are reacted with diisocyanate terminated PU prepolymer through the formation of urea (-NHCONH-) and urethane linkage (-OCONH-). Two new peaks are observed in the NMR spectra at δ = 26.9 and 71 ppm in the graft copolymer corresponding to the prepolymer PU and the peaks corresponding to the chitosan remain unchanged. It is interesting to note that intensities of these new peaks are gradually increases with the increase of reaction time suggesting higher grafting density. The DS is calculated from the deconvulated area of the corresponding NMR peak using equation no. (v) [Ishida et al., 1996].DS is found 10 and 15% for the copolymer formed after 3 and 6 min reaction, respectively. The copolymers are termed as CHT10 and CHT15 where digit after CHT

indicate percentage of substitution shown in **Table4.1**.Grafted copolymers are formed in brush like structure with

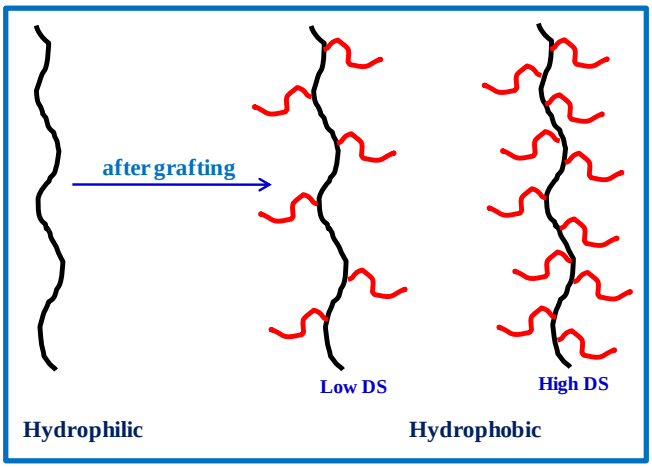

Figure 4.1: Schematic representation of brush copolymer architecture as prepared trough grafting.

Table 4.1: Reaction condition and nomenclature of brush copolymers.

Sample identification	Degree of Substitution	Time of Reaction	
		Step 1. (h)	Step 2. (min)
CHT10	10	2	3
CHT15	15	2	6

different degree of substitution as shown in **Figure 4.1**. The main characteristics peaks of chitosan are observed at 1650 and 1555 cm^{-1} for to >C=O stretching (amide I) and >N-H bending (amide II) of the residual N-acetyl groups, respectively (**Figure 4.2b**) **[**Abureesh et al., 2016**].** Chitosan shows a broad band in the range of 3500-3200 cm^{-1} for combined stretching vibration of hydrogen bonded -O-H and >N-H. The peak at 3339 cm^{-1} for chitosan becomes narrower and has shifted to lower frequency region at 3325 cm^{-1} in both graft copolymer [Kim et al., 2013]. The narrowness of the peak in graft copolymer

is attributed to less inter- and intramolecular hydrogen bonding in graft copolymers as – NH_2 and – OH groups in chitosan molecules are getting converted into urea and

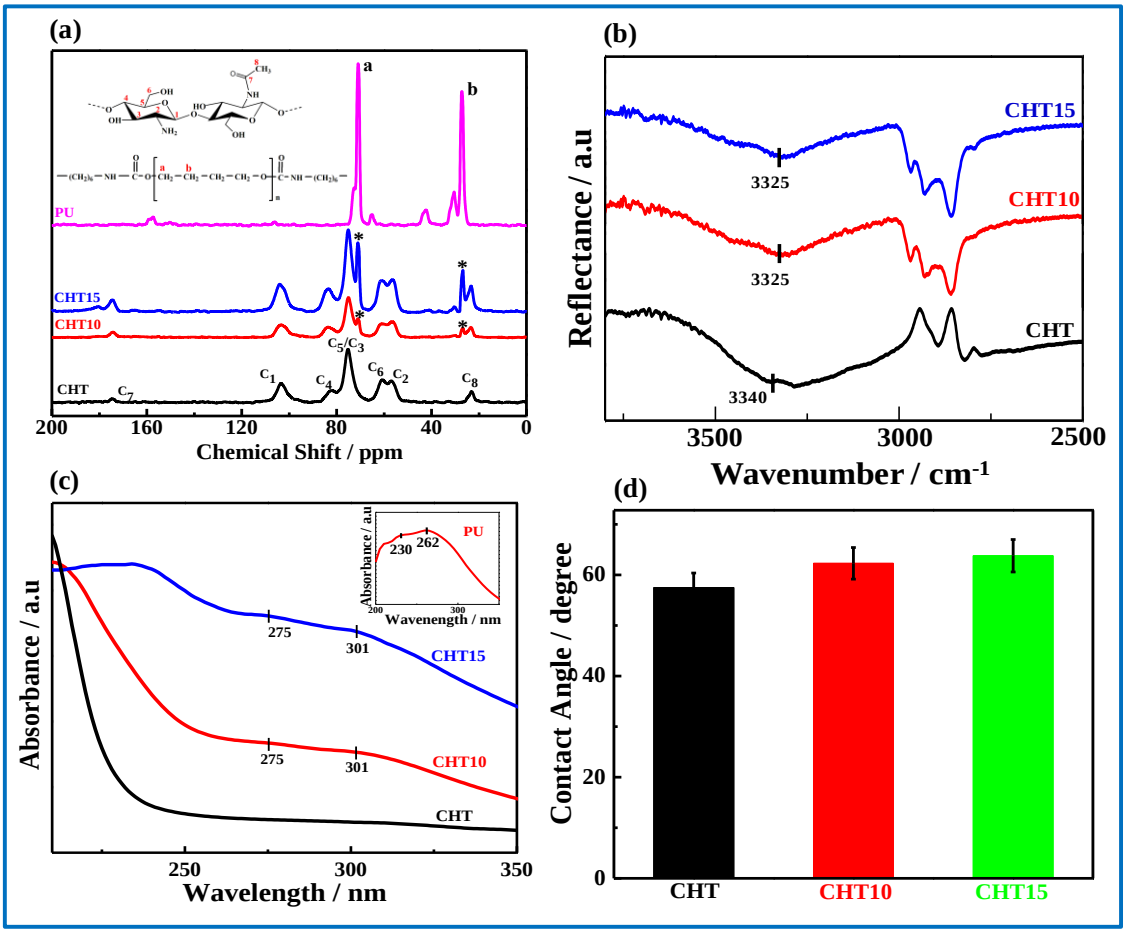

Figure 4.2: (a) ^{13}C Solid State NMR spectra of CHT, PU and their brush copolymer. Selected carbon atoms are assigned according to numbering system given in the structure shown in the inset; (b) FTIR spectra of pure chitosan and its graft copolymers; (c) UV-visible spectra of pure CHT and its indicated graft copolymers; (d) Contact angle of chitosan and its copolymers with different degree of substitution.

urethane linkages after reacting with isocyanate terminated prepolymer PU. The shifting of the band is related to the interaction between grafted PU and chitosan chain through the dipolar interaction. The interaction between PU chains and chitosan chain also observe through UV-visible spectroscopy. The shifting of π–π* and n–π* transitionpeaks from 230 and 262 nm in pure PU, respectively, to 275 and 301 nm in graft copolymer

indicates greater interaction in copolymers (**Figure 4.2c**) [Chen et al., 2005]. Chitosan does not show in absorption peak while pure PU shows two peaks corresponding to the $\pi-\pi*$ and $n-\pi*$ transition.

Grafting of hydrophobic PU chain wrap up the hydrophilic chitosan chain and converted them into hydrophobic as evident from the higher contact angle of graft copolymer (62^o and 64^o for CHT10 and CHT15, respectively) as compared to pure CHT (57^o) (**Figure 4.2d**). Further graft copolymers show two stages thermal degradation as opposed to single stage degradation of pure PU and CHT as shown in TGA thermograms (**Figure 4.3a**). Initial weight loss for absorbed water occurs in the temperature range of 45-115 ^oC and next phase degradation at ~280 ^oC is for the decomposition of chitosan. The degradation at ~400 ^oC is attributed the thermal degradation of PU part present in the copolymers. **Figure 4.3b** shows the DSC thermograms of chitosan and its graft copolymers. A broad peak at ~50 ^oC is observed in DSC thermogram for loss of absorbed water molecules in chitosan while pure PU shows a sharp melting peak at 52 ^oC which has shifted to lower temperature at 42 and 25 ^oC for CHT10 and CHT15, respectively. The shifting is presumably due to the dilution effect and interaction between PU and CHT chains. Interaction leads to the lowering of the melting temperature, and in addition the heat of fusion decrease significantly to 20 and 13 Jg^{-1} for CHT10 and CHT15, respectively, as compared to the value of 76 Jg^{-1} for pure PU also indicate greater interaction between the components. However, DSC results are in good agreement with the spectroscopic conclusion. PU shows two characteristics peaks at $2\theta = 20^o$ and 24.4^o which are present in graft copolymers. The intensities of these peaks are low indicating reduced crystallinity arising from greater interactions (**Figure 4.3c**). Pristine chitosan shows two peaks at $2\theta = 9.54^o$ and 20^o forhydrated crystalline and amorphous structure, respectively [Wang et al., 2016; Chen et al., 2011].

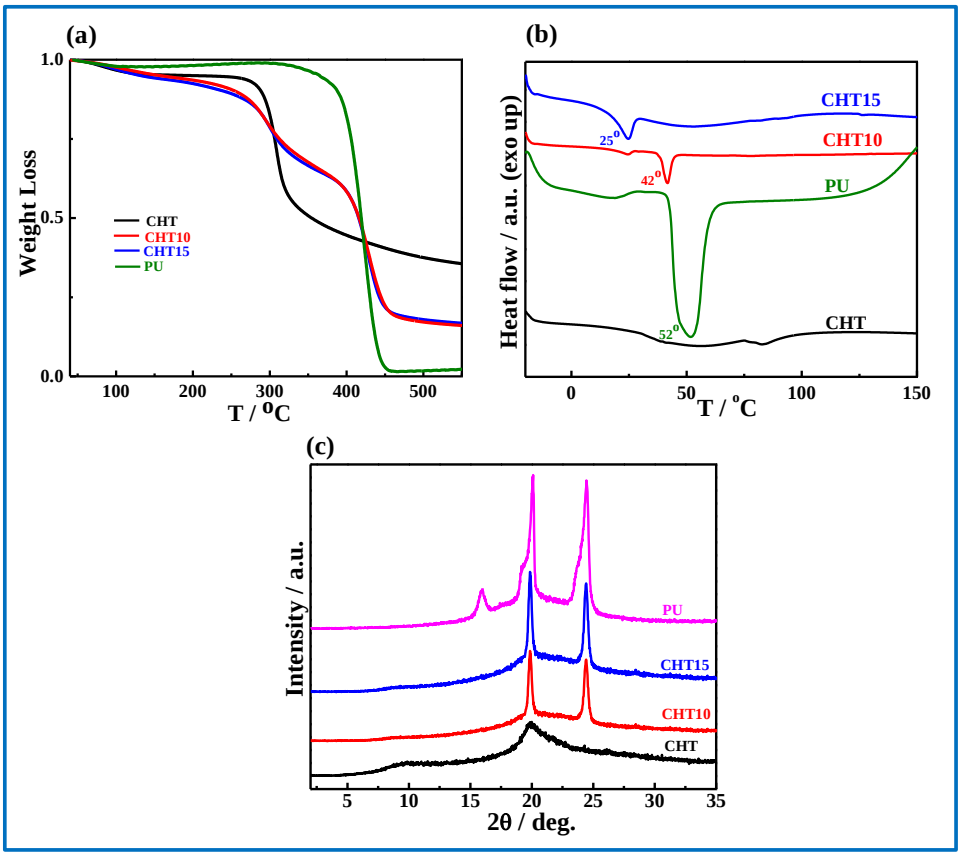

Figure 4.3: (a) Weight loss fraction as function of temperature; (b) DSC thermograms of CHT and its graft copolymers showing the melting temperature; (c) XRD patterns of pure CHT, Pure PU and the indicated graft copolymers.

4.2.2 Gelation and morphology of graft brush copolymer

Chitosan form gel but some difficulties observe as it forms gel solution process and the window for gelation is quite small to work on any practical problem e.g. injectable gel for controlled drug delivery. The gelation of chitosan and its graft copolymers has been studied in 0.1M acetic acid medium and the phase diagram (temperature vs. concentration of gelation) is shown in**Figure 4.4**. Phase diagram indicates larger window for gelation in graft copolymer as opposed to small window for pure chitosan and both the temperature and concentration window has increased for graft copolymers. Pure chitosan at higher concentration remains in a swelling state and thereby put limitation of formation of gel at lower and higher concentration (3>x>6 wt.%) for greater strength. On the other hand, graft copolymers form gel at lower and higher concentration (2-8

wt.%) in addition to high temperature gelation (20-80 ^{o}C). Furthermore, CHT15 shows greater window in terms of temperature and concentration as compared to CHT10 indicating better control of gelation using graft copolymer with its varying degree of substitution. It is believed that pure chitosan show gelation through the formation of inter- and intra-molecular hydrogen bonding which is restricted at higher temperature (60 ^{o}C) and do not form gel at higher temperature. In case of graft copolymers better interaction and network structure help to form gel in a wide range of concentration and temperature. Hence, graft copolymers are promising to form injectable hydrogel against pure chitosan.

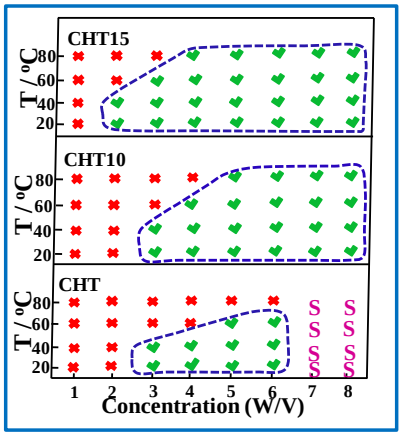

Figure 4.4: Phase diagram (temperature vs. concentration of gelation) of pure CHT and itsindicated graft copolymers where, green marks indicate gel state, red marks indicate sol state, and '**S'** indicates swelled state of polymers and it does not form gel.

The surface morphology of lyophilized hydrogel scaffold of CHT and its graft copolymers are shown in **Figure 4.5a**.The lyophilized hydrogel scaffold exhibit porous structure with interconnected pores and the average pore sizes are 50, 47 and 35 µm for CHT, CHT10 and CHT15, respectively, with narrower distribution in graft copolymer as compared to pure chitosan (**Figure 4.5b**). Scaffold having pores are of great importance for solvent like body fluid affinity or protected cavity for the cells to grow on this substrate. **Figure 4.5c** shows swelling profile of CHT and its graft copolymers are

studied in distilled water at 37 ^{o}C and dried hydrogel specimens were used for swelling studies. Pure chitosan shows very high swelling (Chitosan shows 2000% swelling in just one minute) because of its high hydrophilic nature while graft copolymers show lower percentage of swelling which gradually increase with time. Further, the graft copolymer with high DS like CHT15 show lower percentage of swelling indicating relatively high hydrophobic character supporting the contact angle data. Deswelling profile is shown in Supplementary **Figure 4.5d**.

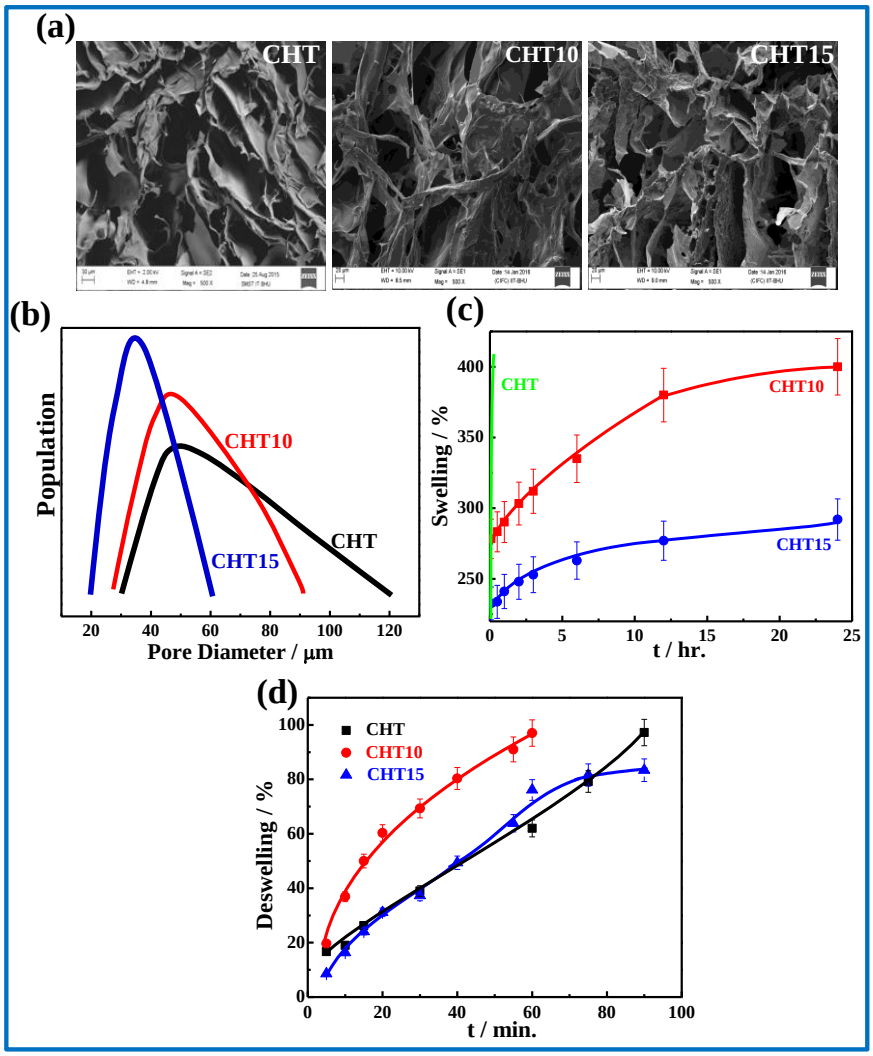

Figure 4.5: (a) SEM images of lyophilized hydrogel of CHT and its indicated graft copolymers showing porous nature of the surface; (b) Pore size distribution of lyophilized hydrogel scaffold of pure chitosan and its indicated copolymers; (c) Swelling profile of CHT and its graft copolymers in distilled water at 37 ^{o}C; (d) Deswelling profile of swollen dried hydrogel film of pure CHT and its indicated copolymers.

4.2.3 Mechanical responses of hydrogel and scaffold- graft density dependency

Mechanical strength of Hydrogel and scaffold are very important for their possible use in biomedical application. The stress-strain curves of CHT and its graft copolymers scaffold under uniaxial compression test showing typical foam behavior of the materials has shown in **Figure 4.6a.** Young's modulus considerably decrease in graft copolymers and the values are of 23, 0.5 and 3.5KPa for CHT, CHT10 and CHT15, respectively. Chitosan is rigid system because of their extensive inter- and intramolecular hydrogen bonding where as lack of sufficient hydrogen bonding in graft copolymers decrease their modulus. However, with higher degree of substitution significant improvement in modulus and toughness is observed like CHT15 shows higher modulus and toughness than CHT10 (**Figure 4.6b and c**).

Hydrogel strength has been measured as a function of frequency under oscillatory shear. Storage modulus, loss modulus and complex viscosities have been shown in **Figure 4.7a.** Storage modulus ($G^{/}$) increases in graft copolymers as compared to pure chitosan and follow the same trend with higher degree of substitution for the entire frequency range.The complex viscosity (η^{*}) of CHT10 initially decreases but a sharp rise in CHT15 is observed indicating higher gel strength of graft copolymer with greater fluiditypredominantly from the brush like network structure where the brushes act as slip agent causing reduced viscosity under shear [Goicochea et al., 2016].**Figure 4.7b** represents the viscosity as a function of temperature which indicates lower viscosity for graft copolymers as compared to pure CHT. Pure CHT has low viscosity beyond 50 ^{o}C is primarily due to breakage of hydrogen bonds which phenomena do not exist for graft

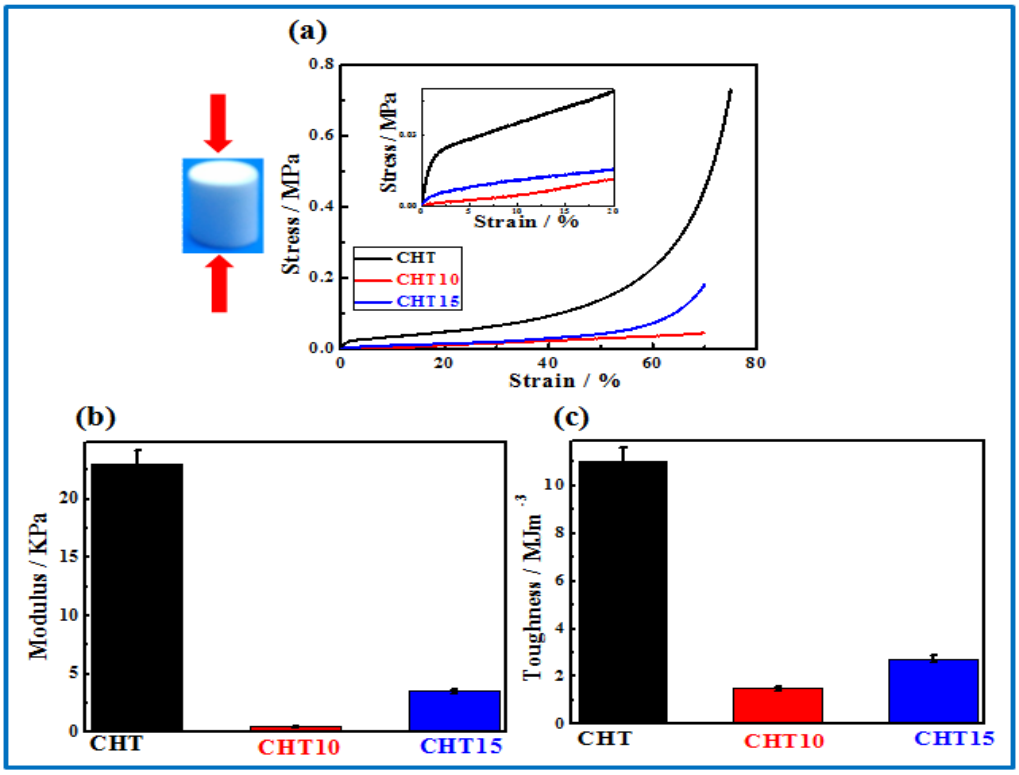

Figure 4.6: (a) Stress-strain curve of the lyophilized hydrogels of CHT and its indicated graft copolymers; (b) and (c) represent the modulus and toughness of the lyophilized hydrogel scaffold of Pure CHT and its indicated copolymers.

copolymer as there is no considerable hydrogen bonding as discussed earlier. CHT10 with low graft density show lower value of viscosity as compared to pure CHT while higher graft density over chitosan chain increases the three dimensional network causing higher viscosity under steady shear (**Figure 4.7c**). However, enhancement in gel strength in graft copolymer with greater fluidity which has potential to be used in biological applications. However, the gel strength increases in graft copolymer with greater fluidity which has potential to be used in biological applications.

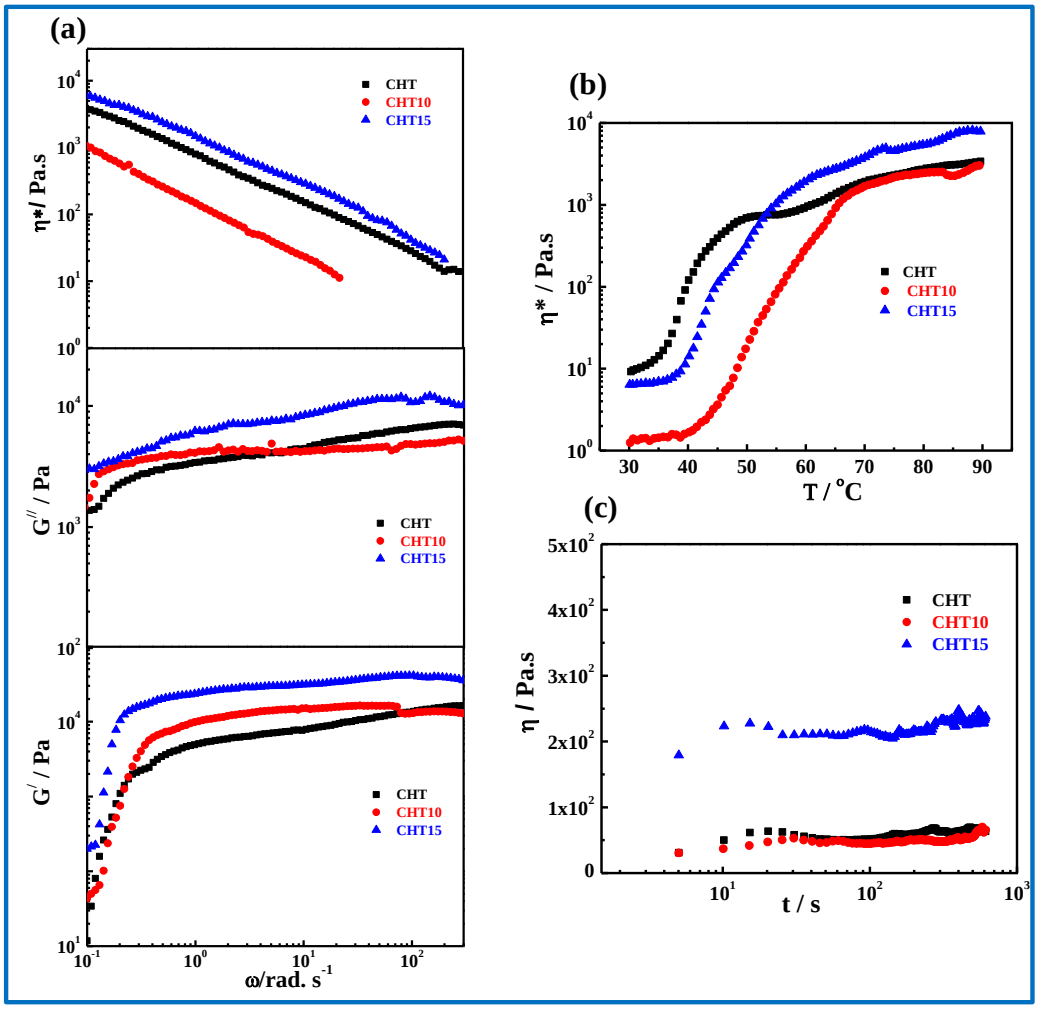

Figure 4.7: (a)Mechanical response of CHT and its indicated copolymer hydrogel in dynamic mode, viscosity (η∗) [top], loss modulus ($G^{//}$) [middle], storage modulus ($G^{/}$) as function frequency under oscillatory shear; (b) Viscosity (η∗) of indicated hydrogel as a function of temperature; and (c) Steady shear viscosity (η) vs. time of indicated hydrogel at 30^{o}C(γ = 0.1 s^{-1}).

4.2.4 In vitro controlled drug release

Gel and scaffold having sufficient mechanical strength can be used as drug delivery vehicle. *Invitro* drug release study is performed in PBS (pH~7.4) medium at 37 ^{o}C maintaining the physiological condition. Tetracycline hydrochloride, antibacterial drug used as a model drug for drug release study. **Figure 4.8 a & b** show the cumulative percent release of the drug as a function of time using hydrogel and scaffold, respectively.

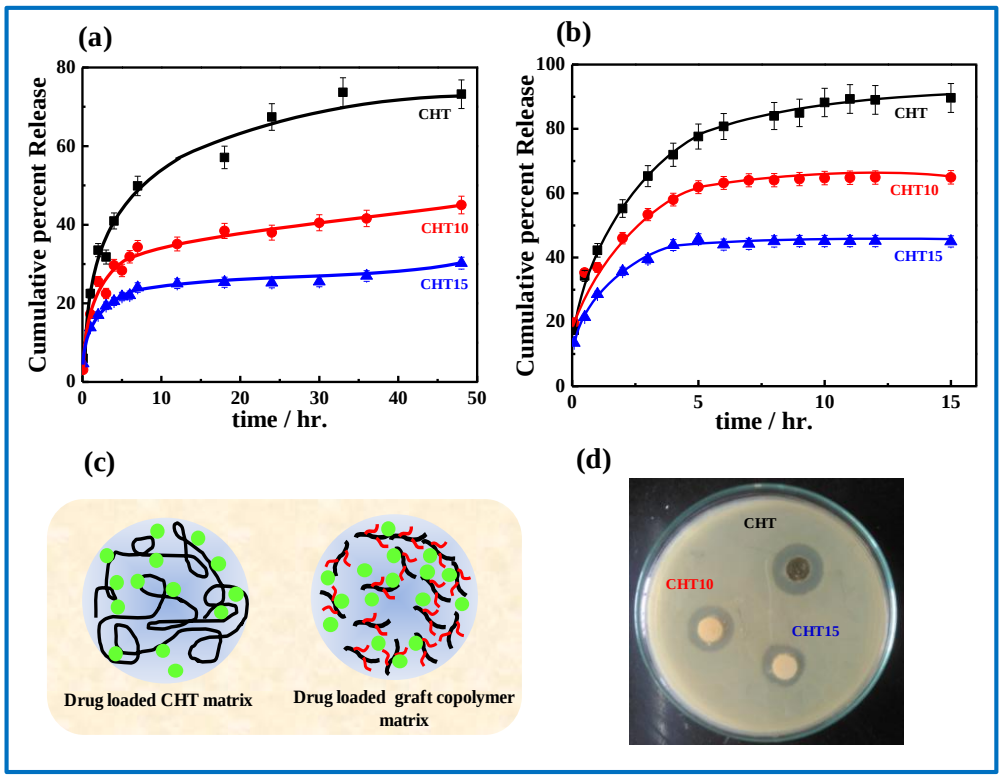

Figure 4.8: Drug release profile of CHT and its indicated graft copolymers showing sustained release for graft copolymers; (a) using hydrogel and (b) using lyophilized hydrogel; (c) Schematic model of drug release kinetics elucidating slow drug release behavior from graft copolymer; (d) Digital photograph of antibacterial activities of indicated hydrogels sample against Gram-negative bacteria, *E. coli* through disc diffusion method.

It is worth mentioning that graft copolymers show sustained release behavior in comparison to pristine CHT in both the cases (gel and scaffold).In case of hydrogel,Pure CHT shows ~75 % drug release in 48 h whereas graft copolymer release 45 and 30 % using CHT10 and CHT15, respectively, in similar time frame. Initial burst release is observed in pure CHT which is completely suppressed in graft copolymers. On the other hand, drug release kinetics from the scaffold is faster than the hydrogel. Pure CHT, CHT10, and CHT15 exhibit total drug release of 90, 65, and 45% in 15 hrs using scaffold. Liquid penetration into the matrix, dissolution of the drug and diffusion of the drug are the most important steps which control the release of drug from polymer matrix and any of them may be the rate determining steps [Singh et al., 2012]. *In vitro*Drug

release kinetics from hydrogel and scaffolds are fitted with different mathematical model and find to be best fitted with the Korsmeyer-Peppas model [Dash et al., 2010; Rai et al., 2016]. The exponent "*n*" values obtained from the Korsmeyer-Peppas model in both cases, mentioned in **Table 4.2a&b**, are $n < 0.45$ indicating Fickian nature of drug diffusion from the pure CHT and its copolymers. A model has been proposed based on the drug release kinetics, where the diffusion of dug molecules is relatively easy from CHT matrix while three dimensional networks in graft copolymer along with strong interaction cause slow diffusion of drug (**Figure 4.8c**). The slow drug release from graft copolymer can also be visualized through the formation of zone of inhibition with drug loaded hydrogel sample against Gram-negative bacteria, *E. coli*through disc diffusion method (**Figure 4.8d**). It is observed that zone of inhibition formed by the graft copolymers is small as compared to the pure CHT and the observed zones of inhibition are 3, 2.4 and 2 cm for pure CHT, CHT10 and CHT15, respectively. To understand the reason of slow drug release from graft copolymers, different Spectroscopic techniques and thermal studies have been performed. The characteristic peaks exhibit by pure drug are C=C vibration of aromatic ring at 1458 cm-1 and NH_2 deformation of amide II at 1542 cm^{-1} and their appearance in the drug loaded samples confirm the presence of drug in scaffold (**Figure 4.9a**) [Senapati et al., 2016]. The N-H and O-H absorption bands are appeared in 3465-3441 cm^{-1} region and here pure drug shows such band at 3447 cm^{-1}. The shifting of the peak is greater for copolymers. Drug embedded specimens show the peak at 3447, 3434 and 3427 for CHTD, CHT10D and CHT15D, respectively, indicating strong interaction between drug and copolymers as compared to pure CHT (**Figure 4.9b**). Furthermore, relatively greater interaction is observed with high graft density copolymer like CHT15 ac compared to CHT10 which is responsible for sluggish release rate in CHT15. Greater interaction between drug and copolymers also observe through UV-

Table 4.2: Release rate constant (*k*), correlation coefficient (r_2) and diffusion releaseexponent (*n*) obtained using different mathematical model from the drug release kinetics using hydrogel (a) and scaffold (b) of pure chitosan and its indicated copolymers.

(a)

Sample	Zero Order		First Order		Higuchi		Korsmeyer-Peppas	
	K	r^2	*K*	r^2	*K*	r^2	*n*	r^2
CHT	4.26 ± 0.76	0.88	0.051 ± 0.012	0.79	16.04 ±2.39	0.91	0.40 ± 0.002	0.98
CHT10	2.59 ± 0.66	0.78	0.043 ± 0.013	0.70	9.82 ± 2.20	0.71	0.35 ± 0.008	0.99
CHT15	1.60 ± 0.24	0.91	0.036 ± 0.007	0.84	6.11 ± 0.40	0.70	0.28 ± 0.009	0.99

(b)

Sample	Zero Order		First Order		Higuchi		Korsmeyer-Peppas	
	K	r^2	*K*	r^2	*K*	r^2	*n*	r^2
CHT	8.74 ± 0.89	0.95	0.064 ± 0.009	0.91	28.78 ±1.05	0.87	0.38 ± 0.006	0.99
CHT10	6.19 ± 0.64	0.95	0.054 ± 0.008	0.91	20.39 ± 0.8	0.91	0.32 ± 0.006	0.99
CHT15	4.23 ± 0.51	0.94	0.049 ± 0.007	0.90	13.98 ±0.82	0.74	0.29 ± 0.008	0.99

visible spectroscopic technique (**Figure 4.9c**). Pure drug shows two peaks at 277 and 358 nm, respectively for π–π* and n–π* transition and shifted to lower wave length as compared to pure drug indicating greater interaction between drug and copolymer as compared to drug and pure CHT [Ghadim et al., 2013]. The greater shifting in CHT15D as compared to the CHT10D is related to the greater interaction of drug with the high graft density copolymer. Thermal behavior of the drug loaded sample (CHTD, CHT10D and CHT15) along with pure drug (D) has been investigated with differential scanningcalorimetry and their corresponding thermograms are shown in **Figure 4.9d**. Elevation of melting point and enhancement in the heat of fusion (ΔH) are observed for the drug loaded copolymers due to nucleating effect drug. Pure drug show an

endothermic peak at 230 ^{o}C is attributed to the melting temperature of the drug followed by an exothermic peak for oxidation (**Figure 4.9e)** [Fernandes et al., 1999].

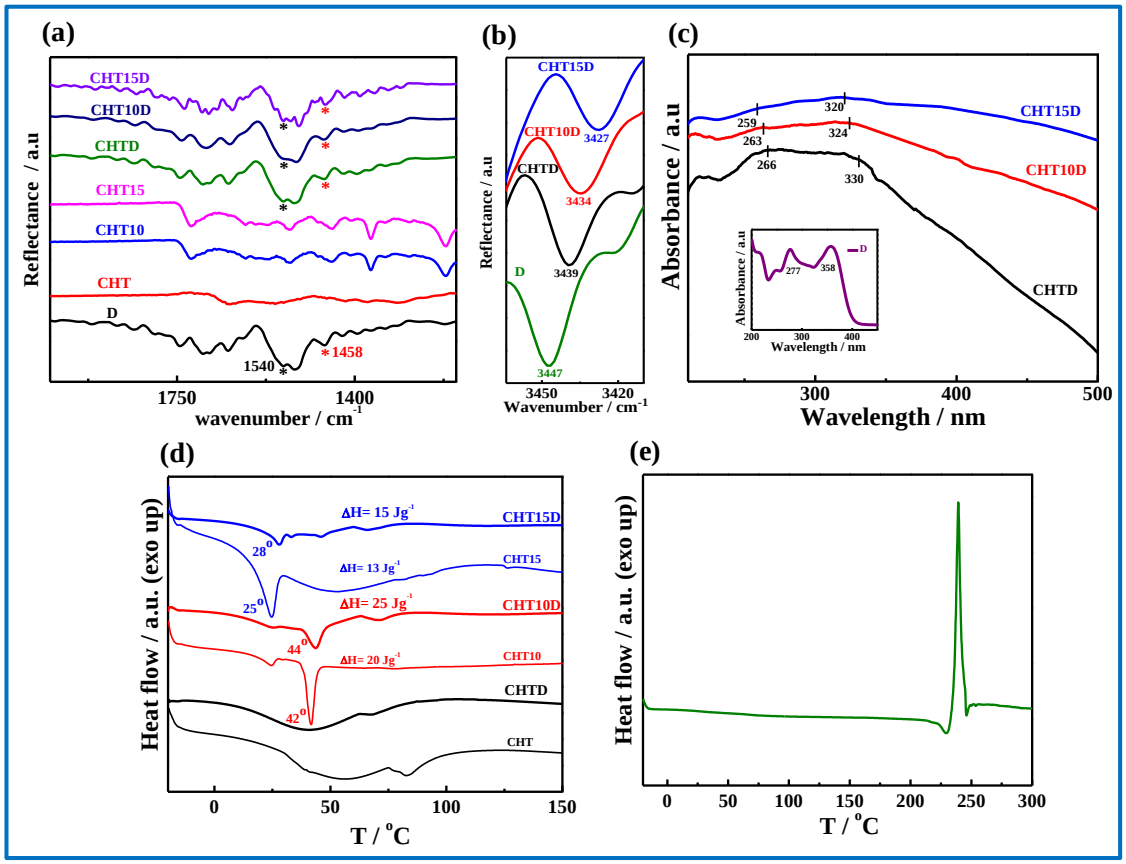

Figure 4.9: (a) FTIR spectra of pure drug, pure chitosan and graft copolymers along with their corresponding drug embedded sample. Asterisks mark indicates the peak position.; (b) FTIR spectra of drug embedded CHT and its graft copolymers, D represents pure drug and D after sample name indicates corresponding drug embedded sample; (c) UV-visible spectra of pure drug and drug embedded sample, CHTD, CHT10D and CHT15D represent the drug embedded chitosan and its graft copolymer, respectively; (d) DSC thermograms of chitosan and graft copolymers along with their corresponding drug loaded sample; (e) DSC thermogram of pure antibiotic drug, tetracycline hydrochloride.

However, slow drug release kinetics from the graft copolymer as compared to the pure Chitosan is mainly due to the greater interaction and network structure either in gel and scaffold form of specimen and graft copolymer is found to be a novel delivery vehicle for control release of drug.

4.2.5 Cytotoxicity

Any materials for using as biomaterial in general and drug delivery vehicle in particular must be nontoxic in nature. The cytotoxicity of material can be checked through the viability of cells over the materials. Cell viability of NIH 3T3 cells on hydrogel and scaffold has been observed through MTT assay at different time interval. The cell viability of pure CHT and its graft copolymers using hydrogel and scaffold has been shown in **Figure 4.10a&b.** Cells treated without specimen taken as control. Graft copolymer show greater cell viability as compared to pure CHT but overall viability increases with time for all specimens indicating graft copolymers as better biocompatible material vis-à-vis pure CHT. Furthermore, scaffold has relatively higher cell viability as compared to hydrogel suggesting scaffolds as better biocompatible material. Brush polymer with high graft density (CHT15) exhibits greater biocompatibility both in hydrogel and scaffold for the entire time scale studied.Fluorescence images of the cells proliferated on hydrogel and scaffold during MTT assay also support the higher cell density in graft copolymers as compared to CHT indicating better biocompatible nature of graft copolymers (**Figure 4.10c&d**). In order to understand the cell proliferation on scaffold, cells are seeded onto various scaffolds. Cells are proliferated on the surface of the CHT scaffold while most of the cells are grown in the interior parts of the pores in the grafted scaffold (**Figure 4.10e**). However, cells are mostly found inside the pores of graft/brush scaffolds where suitable cellular framework for the cell proliferation against surface grown phenomena in CHT scaffold.

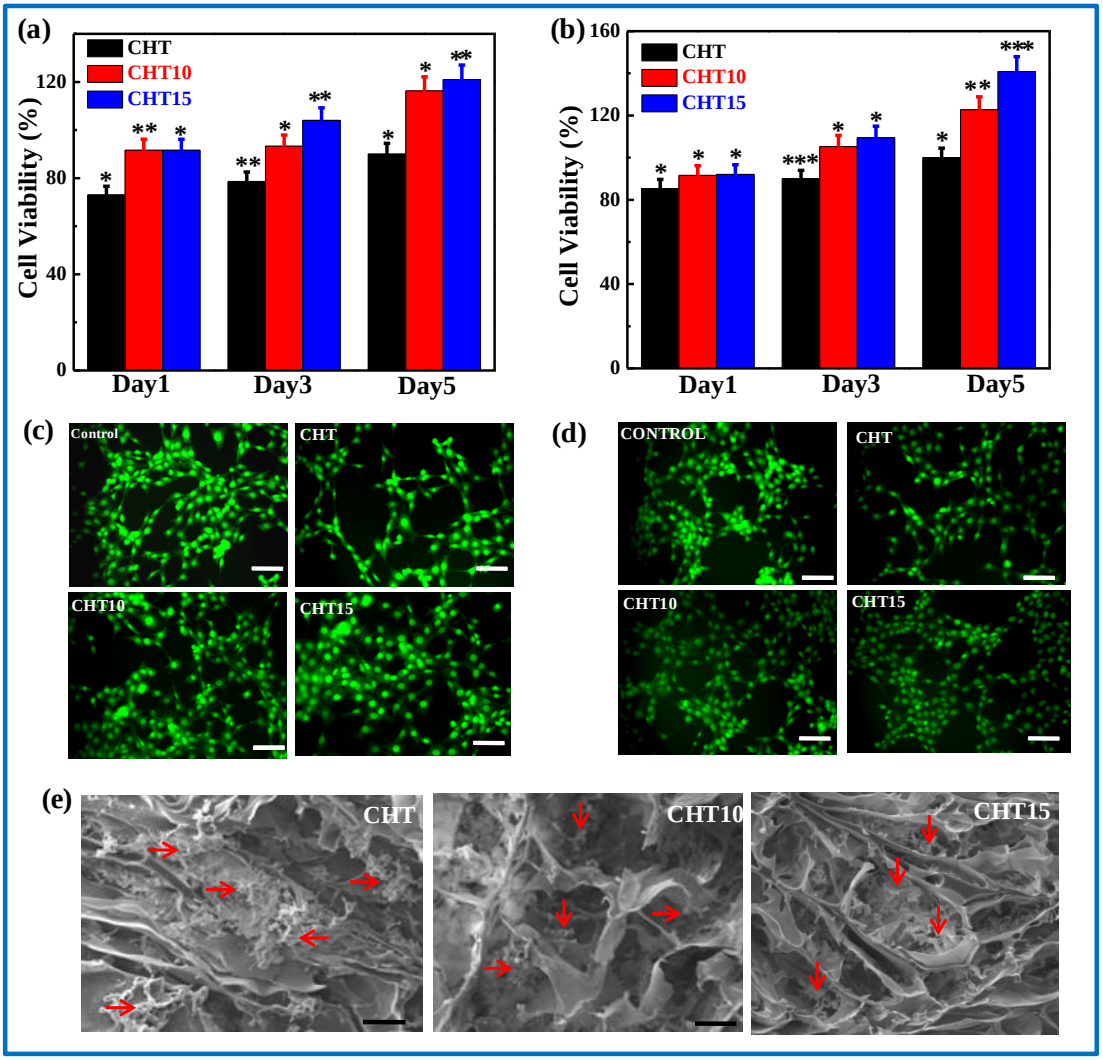

Figure 4.10: Cell viability of pure CHT and its indicated graft copolymer with time interval of 1, 3, and 5 days using (a) hydrogel, and (b) lyophilized hydrogel; All the results presented are mean ± standard deviation values obtained from three independent experiments, where *P < 0.05, **P < 0.01, and ***P < 0.0001. Fluorescence microscopic images of cell cultured on indicated sample after 5 day of cell proliferation using (c) hydrogel, and (d) lyophilized hydrogel. Scale bar = 45µm; (e) SEM image of cell seeded lyophilized hydrogel of pure CHT and it's indicated graft copolymers. Red arrows indicate the position of cells inside the lyophilized hydrogel. Scale bar = 60 µm. Cells have grown within the porous structure in graft copolymer while it grows on the surface of chitosan porous lyophilized hydrogel.

4.2.6 In vivo gelation study in rat model

Although Chitosan form hydrogel but its instant gelling process restricts its use as an injectable hydrogel for biomedical application but brush like graft copolymer form

hydrogel gradually as a function of time, depending on the concentration and temperature, can be used as injectable hydrogel. Graft copolymer with higher DS (CHT15) has been chosen to check in vivo gelation. 1 ml of sol of the said copolymer is

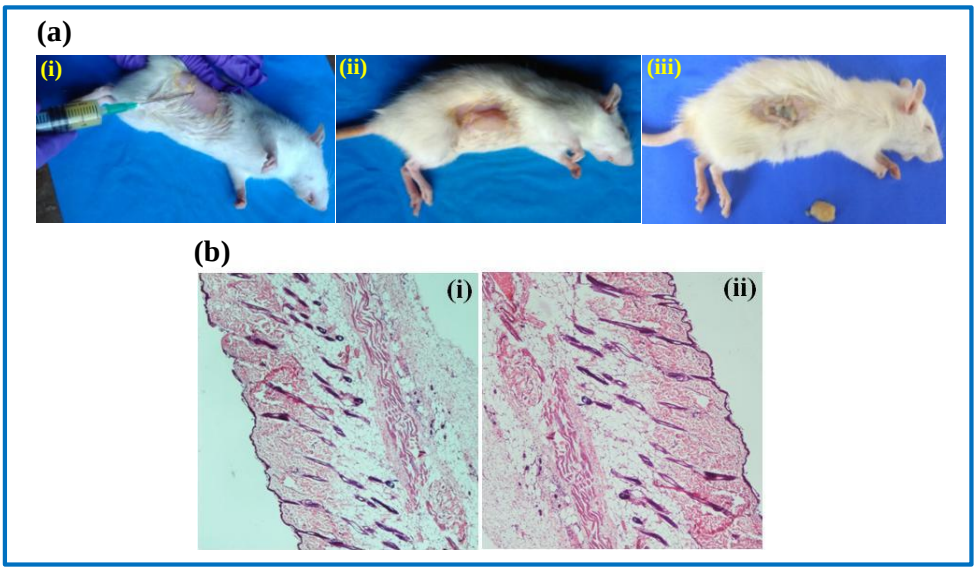

Figure 4.11: *In vivo* gelation study in SD rat model. (a); (i) During injection, (ii) after 15 min of injection showing considerable swelling due to gelation under the skin and (iii) after 24 hrs of injection formed hydrogel has been peeled out; and (b) histopathology of the skin, where (i) represents 'control' without injected materials and (ii) represents the skin of hydrogel forming area.

injected on the right dorsal side of rat and images are captured to visualize the formation of hydrogel under dermis. After 15 minutes of subcutaneous injection hydrogel formation can be visualized by the considerable swollen image of the location where injection was given under the subdermal mucous layer (**Figure 4.11a (i) and (ii)**). Hydrogel has been peeled out from the subdermal mucous layer after 24 hours of gel formation shown in **Figure 4.11a (iii)**. Pathological tissue section (Skin) is taken from the hydrogel forming site after 24 hrs of injection of the materials (**Figure 4.11b**) and histopathological examination reveals that there is no side effect/inflammation on tissue in presence of hydrogel.We have tried to develop injectable hydrogel of chitosan without gelator but its

high solubility converts it to hydrogel instantly above the concentration of 2.5 % (w/v). There are several literature reports on injectable hydrogel using different gelators while polyurethane grafted chitosan brush copolymer can serve the purpose successfully without using any kind of gelator [Wang et al., 2016; Li et al., 2014; Wang et al., 2017].

4.3 Conclusion

Hydrophilicity of chitosan has been modified through grafting of polyurethane chain onto its backbone developing brush like structure for its possible application in biomedical arena. Diisocyanate terminated polyurethane chains have been grafted with different degree of subtiution for chemical modification of chitosan. The grafting is confirmed through solid state NMR and degree of substitution is determined from the corresponding NMR spectrum. Other spectroscopic techniques like FTIR and UV-visible are also used to understand the interaction between components as evident from the shifting of the peak positions and depression of melting temperature. Hydrophobic modification of chitosan is confirmed from increase contact angle and decrease in swelling characteristics of graft copolymers in comparison to pure CHT. Graft copolymers are fabricated to hydrogel and scaffold with and without drug in it. Phase diagram of the gelation as function of concentration and temperature shows greater window for graft copolymer as compared to pure CHT. Mechanical strengths of the hydrogel/scaffold have been evaluated showing higher storage modulus but lower viscosity of the graft copolymer. Low viscosity is observed presumably due to brush like structure which act as slip agent causing reduction of viscosity. Graft copolymers are capable of releasing drug in sustained manner as compared to pure chitosan using both hydrogel and scaffold following the Fickian diffusion kinetics. Graft copolymers are well biocompatible in nature as compared to pure chitosan observed through its activity on 3T3 fibroblast cells. Cells are grown inside the pores of the scaffold of graft copolymer where as in pure

chitosan cells are mostly grown on the surface. Sol of graft copolymer injected subcutaneously in rat to demonstrate the hydrogel formation for their possible use as injectable hydrogel. In vivo gelation is observed within 15 minutes. Therefore polyurethane graft chitosan brush hydrogel and scaffold has tremendous potential for future application in drug delivery and tissue engineering.